AMERICAN SOCIETY FOR MICROBIOLOGY | Applied and Environmental Microbiology

Alginate Biosynthesis Factories in *Pseudomonas fluorescens*: Localization and Correlation with Alginate Production Level

Susan Maleki, Eivind Almaas, Sergey Zotchev, Svein Valla, Helga Ertesvåg

Department of Biotechnology, NTNU Norwegian University of Science and Technology, Trondheim, Norway

***Pseudomonas fluorescens* is able to produce the medically and industrially important exopolysaccharide alginate. The proteins involved in alginate biosynthesis and secretion form a multiprotein complex spanning the inner and outer membranes. In the present study, we developed a method by which the porin AlgE was detected by immunogold labeling and transmission electron microscopy. Localization of the AlgE protein was found to depend on the presence of other proteins in the multiprotein complex. No correlation was found between the number of alginate factories and the alginate production level, nor were the numbers of these factories affected in an *algC* mutant that is unable to produce the precursor needed for alginate biosynthesis. Precursor availability and growth phase thus seem to be the main determinants for the alginate production rate in our strain. Clustering analysis demonstrated that the alginate multiprotein complexes were not distributed randomly over the entire outer cell membrane surface.**

Alginates are a group of industrially important unbranched, negatively charged polymers consisting of variable ratios of β-D-mannuronate (M) and α-L-guluronate (G) residues linked by 1-4 glycosidic bonds. Currently, all commercially available alginate is manufactured from marine seaweeds, and the isolated polysaccharides are utilized in various biomedical and industrial applications (1). The M/G composition of alginate displays environmental and seasonal fluctuations (2), and some desired compositions cannot be extracted from algae in sufficient quantities. Some bacteria belonging to the genera *Azotobacter* and *Pseudomonas* have the potential to synthesize alginate with more tailored compositions and without seasonal variations (3). An understanding of bacterial alginate biosynthesis is further of vital importance in medicine because of its particular relevance for the treatment of cystic fibrosis (CF) patients suffering from bacterial infections caused by *Pseudomonas aeruginosa*, an opportunistic human pathogen. *P. aeruginosa* displays a mucoid phenotype due to overproduction of alginate in CF patients' lungs, making treatment of such infection extremely difficult due to the inability of antibiotics to penetrate the alginate layer surrounding the bacteria (4).

In *Pseudomonas*, all proteins—AlgD, Alg8, Alg44, AlgK, AlgE, AlgG, AlgX, AlgL, AlgI, AlgJ, AlgF, and AlgA—directly involved in alginate polymerization, acetylation, epimerization and export are encoded by genes transcribed from the *algD* promoter and from internal promoters (5, 6). One additional gene, *algC*, encoding a bifunctional enzyme with phosphomannomutase and phosphoglucomutase activities, is located distantly from the alginate operon and expressed from its own promoter. AlgC is essential for alginate biosynthesis but is also involved in the biosynthesis of other polysaccharides (7). A set of enzymatic reactions catalyzed by the cytoplasmic enzymes AlgA, AlgC, and AlgD leads to production of the activated alginate precursor GDP-mannuronic acid from fructose-6-phosphate (F6P), which is a key metabolite of the central carbon metabolism (7–10). GDP-mannuronic acid is then polymerized into polymannuronan by the action of the glycosyltransferase Alg8 and the copolymerase Alg44, which contains a c-di-GMP-binding PilZ domain (11). In the periplasm, M residues can be epimerized to G by AlgG (12). They may also be acetylated selectively at O-2′ and/or O-3′ positions by AlgX (13). Additionally, AlgI, AlgJ, and AlgF are involved in alginate acetylation (14, 15). The alginate-degrading enzyme AlgL prevents alginate accumulation in the periplasm, which can be detrimental to the cell (16).

Several studies have indicated that the newly synthesized polymannuronate chain needs to be translocated across the periplasm with the aid of a protein scaffold composed of Alg8, Alg44, AlgG, AlgX, AlgK, and AlgE (17–23). AlgK is a periplasmic lipoprotein bound to the outer membrane and is important, but not essential, for the localization of the porin AlgE. Figure 1 represents the proposed model for alginate biosynthesis machinery based on recent studies (13, 21, 22). The interactions between different Alg proteins, assumed to contribute to the formation of the mentioned protein scaffold, have been extensively studied by mutual stability and pulldown analyses. According to these findings, AlgX plays a crucial role in the localization of the porin AlgE (21). The absence of any of the scaffold proteins AlgG, AlgX, AlgK, or AlgE in a complex leads to release of alginate in the periplasm, where it is degraded by AlgL, resulting in a lower polymer yield (1, 16–20, 24).

To be able to engineer strains for bacterial bioproduction of tailor-made alginates, it is important to better understand the localization of the alginate biosynthesis complexes and factors that would affect their assembly and to determine alginate yield limiting factors. To address this, we have chosen *P. fluorescens* SBW25, which is a nonpathogenic plant-commensal strain investigated in

Received 24 September 2015 **Accepted** 3 December 2015

Accepted manuscript posted online 11 December 2015

Citation Maleki S, Almaas E, Zotchev S, Valla S, Ertesvåg H. 2016. Alginate biosynthesis factories in *Pseudomonas fluorescens*: localization and correlation with alginate production level. Appl Environ Microbiol 82:1227–1236. doi:10.1128/AEM.03114-15.

Editor: V. Müller, Goethe University Frankfurt am Main

Address correspondence to Helga Ertesvåg, helga.ertesvag@ntnu.no.

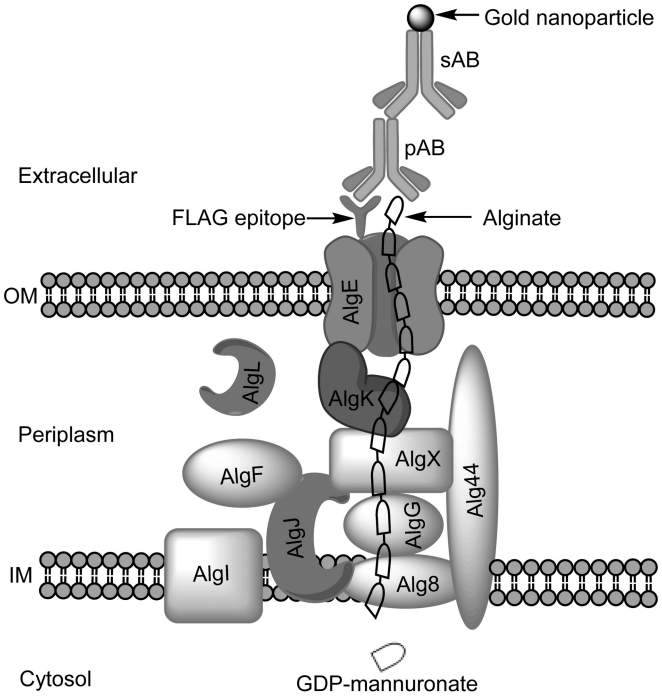

FIG 1 Proposed model for the alginate biosynthesis factory and overview of immunogold labeling of the AlgE-FLAG-tagged protein. In the immunogold labeling method developed in this study, the FLAG epitope tag inserted into the AlgE protein is recognized by the anti-FLAG M2 monoclonal primary antibody (pAB), which is subsequently detected by the gold-conjugated secondary antibody (sAB). It has been proposed that the multiprotein complex, involved in alginate polymerization and secretion, is stretched across the periplasm, conducting the recently synthesized alginate chain to the porin AlgE and finally out of the cell. The order of and interaction between AlgE, AlgK, AlgX, AlgG, Alg8, and Alg44 have been depicted based on the recent studies reviewed by Hay et al. (3). The peptidoglycan layer in the periplasm has been removed, and the cartoon is not drawn to scale. OM, outer membrane; IM, inner membrane.

our group for industrial production of alginate (16, 25). *P. fluorescens* wild-type strains do not naturally produce alginate under laboratory conditions. The mucoid phenotype conversion occurs usually by introducing a point mutation in the regulatory protein MucA, which is an anti-sigma factor negatively regulating the *algD* operon by sequestering the sigma factor AlgU (σ^{22}) required for alginate production (26). It has been shown that the transcript levels of *algC* and of the genes in the alginate biosynthetic operon are significantly upregulated in *P. fluorescens* SBW25 *mucA* compared to the wild-type strain (25). We developed an immunogold labeling procedure for direct detection of the alginate biosynthesis factories using transmission electron microscopy (TEM) in which AlgE, as an indication of the presence of factories, was FLAG-tagged in loop 6 (Fig. 1). Hay et al. have previously demonstrated that insertion of this epitope in loop 6 does not affect alginate production in *P. aeruginosa* (19). Using this approach, we investigated the correlation between the number of factories and alginate production level, their dependence on the production of alginate precursor, and the spatial distribution pattern of alginate factories on the cell surface.

MATERIALS AND METHODS

Bacterial strains and growth conditions. The bacterial strains and plasmids used in this study are listed in Table 1. Routine growth of *Escherichia coli* and *Pseudomonas fluorescens* strains was carried out in L broth (10 g/liter tryptone, 5 g/liter yeast extract, 5 g/liter NaCl) in 250-ml shake flasks at 225 rpm at 37 and 30°C, respectively. For growth experiments, alginate production, and TEM, 1% precultures of respective bacterial strains were inoculated in DEF3 minimal medium (28), containing fructose as carbon source. When appropriate, antibiotics were added in the following concentrations: triclosan (Tric), 25 μg/ml; apramycin (Am), 50 μg/ml; ampicillin (Ap), 200 μg/ml; kanamycin (Km), 50 μg/ml; and tetracycline (Tc), 15 μg/ml. Proteases (0.15 ml/liter of Alcalase 2.4L and Neutrase 0.5L) were added to the alginate production media to avoid degradation of alginate by lyases. Expression from the *Pm* and *Pm-G5* promoters was induced by adding *m*-toluate to 0.25 mM. Conjugation between *E. coli* and *P. fluorescens* strains was carried out on L agar (L broth containing 15 g/liter agar), and transconjugants were selected on *Pseudomonas* isolation agar (PIA; Difco) with the addition of proper antibiotics (1). For the detection of LacZ activity, 60 μl of X-Gal (5-bromo-4-chloro-3-indolyl-β-D-galactopyranoside) solution (20 mg/ml in dimethyl sulfoxide) was added to each agar plate 30 min before the plating of bacteria. Alginate was harvested and quantified using M- and G-specific lyases as described earlier (28–30). All alginate quantifications were performed using three technical replicates. Standard deviations were estimated using the sample standard deviation formula on biological replicates.

Construction of AlgE-FLAG epitope insertion mutant strains. General DNA cloning and manipulation procedures were performed as described previously (16). The *E. coli* strains S17.1 and S17.1(λ*pir*) were used as plasmid hosts. All amplified DNA fragments were confirmed by DNA sequencing.

Plasmid pSM8 in which the FLAG (DYKDDDDK) epitope-coding nucleotide sequence (31) was inserted into *algE* was constructed using PCR. Two PCR products targeting *algE* gene were generated using *P. fluorescens* genomic DNA as the template: one with P1 and P2 (amplifying a fragment containing the end of *algK* and the 5′ part of *algE* until bp 864 of the open reading frame [ORF]) and the other one with P3 and P4 (amplifying a fragment containing the 3′ part of the gene from bp 865 of the ORF and the beginning of *algG*) primer pairs. A total of 24 bp encoding the FLAG epitope and the complementary sequence were inserted at the 5′ end of primers P3 and P2, respectively. To be able to confirm the correct insertion of FLAG-coding DNA sequence by PCR and restriction enzyme digestion, an Acc65I restriction site was introduced into the primer pair P2 and P3 by changing a cytosine (nucleotide 867 of *algE*) to a thymine; the corresponding codon still encodes a glycine. The two PCR products were then mixed in equimolar amounts and used as the template for a third PCR with the P1 and P4 primers. The resulting PCR product contained the FLAG epitope, inserted after bp 864 of *algE*. The purified product was then cloned into EcoRV-digested pUC128 vector, resulting in pSM7. Finally, XbaI-NsiI-digested *algE*-FLAG fragment (2.0 kb) was cloned into a gene replacement vector, and the new plasmid was designated pSM8.

pSM8 was then used to generate chromosomal FLAG epitope insertion variants (listed in Table 1) as described elsewhere (1). All constructed strains were verified by PCR amplification and restriction digestion.

In order to express the FLAG-tagged AlgE protein in *P. fluorescens* SBW25, a transposon vector, where the *algE*-FLAG was placed under the control of the inducible *Pm-G5* promoter (32) was constructed (Table 1). This plasmid was designated pSM9 and transferred into *P. fluorescens* SBW25 by conjugation. Transposon insertion mutants were selected on PIA containing Am. Several transposon mutants were initially checked in order to avoid selecting recombinant strains in which the phenotype is caused by transposon insertion site and not by the expressed gene.

Analysis of AlgE protein production by Western blotting. The cells were grown overnight in DEF3 medium with appropriate antibiotics and then harvested by centrifugation at 5,000 rpm for 5 min. A 10-mg pellet (wet weight) was diluted and used for further processing. Diluted samples were electrophoretically separated on SDS-polyacrylamide gels according

TABLE 1 Bacterial strains and plasmids used in this study

Strain or plasmid	Characteristics[a]	Source or reference
Strains		
E. coli		
S17.1	RP4 2-Tc::Mu-Km::Tn*7* *pro res mod*$^+$	43
S17.1(λ*pir*)	λ*pir recA thi pro hsdR*$^-$*M*$^+$RP4 2-Tc::Mu-Km::Tn*7*TpRSMR	44
P. fluorescens		
SBW25	Nonmucoid wild type; Tric^r	38
SBW25 *algE*-FLAG	Derivative of SBW25 in which a 24-bp insertion encoding the FLAG epitope was inserted after bp 864 of the ORF using pSM8; Tric^r	This study
SBW25::Tn*algE*-FLAG	Derivative of SBW25 in which *algE*-FLAG was expressed by inserting the transposon from pSM9; Tric^r Am^r	This study
SBW25 *mucA*	Derivative of SBW25 containing a truncated version of *mucA*; Tric^r	25
SBW25 *mucA algE*-FLAG	Derivative of SBW25 *mucA* in which a 24-bp insertion encoding the FLAG epitope was inserted after bp 864 of the ORF using pSM8; Tric^r	This study
SBW25 *mucA* Δ*algC*	Derivative of SBW25 *mucA* where pKB22 was used to delete parts of *algC*; Tric^r	25
SBW25 *mucA* Δ*algC algE*-FLAG	Derivative of SBW25 *mucA* Δ*algC* in which a 24-bp insertion encoding the FLAG epitope was inserted after bp 864 of the ORF using pSM8; Tric^r	This study
SBW25 MS1	Derivative of SBW25 where the expression of the alginate operon was controlled by the *Pm* promoter	Mona Senneset, unpublished data
SBW25 MS1 Δ*algC*	Derivative of SBW25 MS1 where pKB22 was used to delete parts of *algC*; Tric^r	Mona Senneset, unpublished data
SBW25 MS1 Δ*algC algE*-FLAG	Derivative of SBW25 MS1 Δ*algC* in which a 24-bp insertion encoding the FLAG epitope was inserted after bp 864 of the ORF using pSM8; Tric^r	This study
SBW25 MS1 Δ*algC algE*-FLAG::TnKB60	Derivative of SBW25 MS1 Δ*algC algE*-FLAG where *algC* was expressed by inserting the transposon from pKB60; Tric^r Km^r	This study
Plasmids		
pYQ1	Derivative of pKD20 where the kanamycin resistance gene was replaced by a gene encoding apramycin resistance (Am^r)	28
pKB60	A transposon vector encoding the transposon TnKB60 in which *algC* is under the control of *Pm-G5*; Ap^r Km^r	16
pMG48	RK2-based gene replacement vector; Ap^r Tc^r	1
pUC128	High-copy-no. ColE1-based cloning vector; Ap^r	45
pSM7	Derivative of EcoRV-restricted pUC128 in which a 1.9-kb PCR fragment containing *algE*-FLAG was inserted; Ap^r	This study
pSM8	Derivative of pMG48 where an XbaI site was introduced and *algE*-FLAG from pSM7 (XbaI-NsiI) was inserted; Tc^r Ap^r	This study
pSM9	Derivative of pYQ1 in which a 1.6-kb NdeI-NotI-PCR fragment from pSM7 encoding *algE*-FLAG was inserted so that *algE*-FLAG was controlled by *Pm-G5*; Am^r	This study

[a] Tric^r, triclosan resistance; Am^r, apramycin resistance; Km^r, kanamycin resistance; Tc^r, tetracycline resistance; Ap^r, ampicillin resistance.

to the Laemmli method (33) using 12% gels and SDS running buffer (ClearPAGE; C.B.S. Scientific). The proteins were either stained with Bio-Safe Coomassie (Bio-Rad) or electrotransferred to an Amersham Hybond 0.45-μm-pore-size polyvinylidene difluoride membrane (GE Healthcare Life Sciences) as described in the manufacturer's protocol. After blotting, the membrane was blocked by 3% skim milk powder (Sigma-Aldrich) in Tris-buffered saline (TBS) for 1 h and washed three times with TBS. Subsequently, the membrane was probed with primary antibody, anti-FLAG M2 monoclonal antibody (Sigma-Aldrich; 1:5,000) and, as the secondary antibody, peroxidase conjugated-goat anti-mouse IgG (Sigma-Aldrich; 1:10,000). The horseradish peroxidase activity was detected by Amersham ECL Prime Western blotting detection reagents (GE Healthcare Life Sciences) according to the manufacturer's protocol.

Immunogold labeling sample preparation, TEM, and image analysis. To be able to visualize FLAG-tagged AlgE protein on the cell surface, an immunogold labeling method was developed and optimized. TEM (JEOL, JEM-1011) was used to examine the presence or absence of the gold-labeled FLAG-AlgE protein on the outer membrane. The whole procedure was carried out at room temperature.

A total of 1 ml of the *P. fluorescens* culture was mixed with 4 ml of phosphate-buffered saline (PBS; 8 g/liter NaCl, 0.2 g/liter KCl, 1.44 g/liter Na_2HPO_4, and 0.24 g/liter KH_2PO_4). To remove alginate, 8 μl (1 U) of each of the G- and M-specific alginate lyases was added to the mixture, which was then incubated for 3 min and centrifuged at 5,000 rpm for 5 min. The pellet was resuspended in blocking buffer (PBS supplemented with 0.05% Tween 20 and 0.3% bovine serum albumin). A 200-mesh Formvar-coated grid was put on the surface of a bacterial suspension drop (50 μl) and kept for 5 min. Excess bacterial suspension was drained off using a clean filter paper, and the grid was air dried for 15 min. The cells attached to the grid, which was then placed face down on a drop of anti-FLAG M2 monoclonal antibody (Sigma-Aldrich; diluted 1:50 in blocking buffer) for 1 h. Afterward, the grids were washed six times, for 5 min each time, with the blocking buffer. The bound antibodies were detected by incubating the grids for 1 h on a drop of anti-mouse IgG gold-conjugated antibody (Sigma-Aldrich) (diluted 1:25 in blocking buffer), followed by the same washing procedure as after the primary antibody. Finally, the cells were fixed on the grids by a 30-min incubation on a glutaraldehyde drop (2% [vol/vol]), rinsed three times with water, and air dried for 15 min before examination by TEM (accelerating voltage of 60 kV). At least three grids were prepared in parallel as technical replicates. All solutions and buffers were sterile filtered.

The images were captured at ×50,000 magnification at regions of the grids where single cells of about the same size were found. The obtained TEM micrographs were analyzed using the iTEM platform. At least 20 to

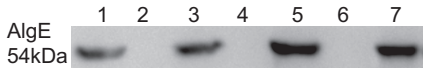

FIG 2 Western blot analysis of samples from the AlgE FLAG epitope insertion variants showing the presence or absence of AlgE. The samples were harvested from overnight grown cell cultures at 30°C, and antibodies were used to detect the FLAG-epitope on AlgE in whole-cell extracts obtained from the following strains: lane 1, SBW25::Tn*algE*-FLAG; lane 2, SBW25; lane 3, SBW25 *mucA algE*-FLAG; lane 4, SBW25 *mucA*; lane 5, SBW25 *mucA* Δ*algC algE*-FLAG; lane 6, SBW25 *algE*-FLAG; and lane 7, SBW25 MS1 Δ*algC algE*-FLAG::TnKB60.

30 random single cells per grid were chosen in order to count the gold particles for statistical analysis, and the average number of particles per single cells was calculated. Microsoft Excel (2010) was used to carry out a Student *t* test analysis.

Numerical image analyses. To investigate the spatial distribution pattern of alginate biosynthesis factories, the coordinates of all gold particles placed within a defined ellipse with axes of 738 and 542 nm, fully included within the image of the cell boundary, were determined for each cell using iTEM platform (Olympus Soft Imaging Solutions). Three types of statistical and numerical analyses were performed as described previously (34), with some modifications:

(i) Nearest-neighbor distance distribution. The nearest-neighbor distance distribution was calculated by measuring the nearest-neighbor distances $NN(r)$ for each particle and plotted using a bin size of 5 nm.

(ii) Ripley's K-test for clustering. The randomness of the spatial distribution of particles over multiple length scales was tested using a modified form of Ripley's K-test. Given that $N(r)$ is the number of particles within a circle with radius r, and D is the average density of particles, then $N(r) = D\pi L^2$, where L is an effective distance. In Ripley's K-test, we define $L(r)$ as follows:

$$L(r) = \sqrt{N(r)/\pi D} \quad (1)$$

If the distribution pattern is truly random, we expect $L(r) = r$ for all values of r. In order to account for effects from both the finite size and the elliptic shape of the sample region, we used computer simulations to determine the random $L(r)$ value $[L(r)_{rand}]$. Consequently, we calculated $L(r)_{exp} - L(r)_{rand}$ for all values of r, where $L(r)_{exp}$ represents the experimental $L(r)$. The standard deviation of the mean was calculated using the expression below:

$$SD_{mean} = \sqrt{(\sigma^{exp}/\sqrt{N_{exp}})^2 + (\sigma^{rand}/\sqrt{N_{rand}})^2} \quad (2)$$

(iii) Nearest-neighbor angle distribution. The angle formed by the lines drawn from a gold particle to its two closest neighbors was calculated and plotted in a histogram using a bin size of 5 degrees.

For each of these numerical analysis approaches, we compared the experimental data to computer-generated control data sets (5,000 sets per analyzed cell) where the same number of particles were randomly distributed in an identically sized and shaped area, the only constraint being that the distance between the simulated particles should be larger than the size of the gold particles (>10 nm).

RESULTS

Production of AlgE-FLAG protein in *P. fluorescens*. To enable visualization of AlgE proteins on the outer membrane using TEM, plasmid pSM8, encoding a mutant protein in which the FLAG epitope (M2) is inserted in the outer membrane loop 6 of AlgE, was constructed. This suicide plasmid is designed to use homologous recombination to replace *algE* with *algE*-FLAG in the *alg* operon. By this strategy, we wanted to minimize the risk of changing the expression level of the outer membrane pore protein.

Plasmid pSM8 was introduced into the strain SBW25 *mucA*, where it replaced the natural *algE* gene, yielding strain SBW25 *mucA algE*-FLAG. The SBW25 *mucA* mutant expresses a truncated form of the MucA protein that is not able to sequester the σ^{22} transcription factor AlgU. Therefore, the alginate biosynthetic operon is constitutively transcribed, leading to stable alginate production (25).

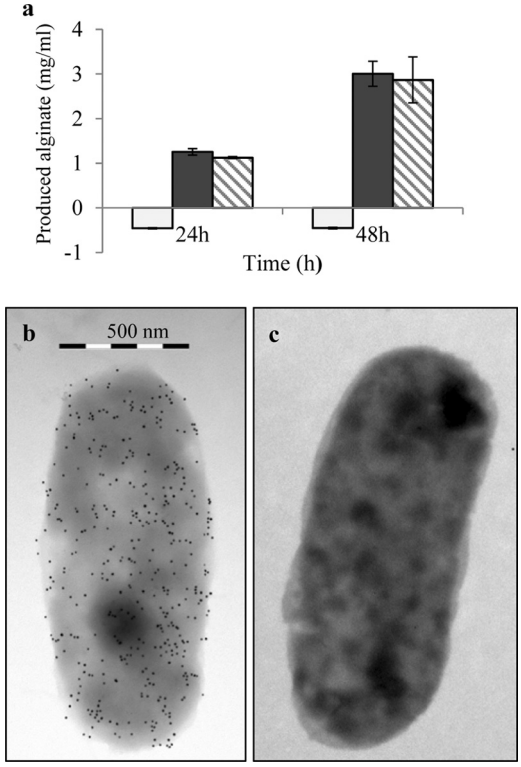

FIG 3 Alginate production and TEM micrographs of strain SBW25 *mucA* and its AlgE-FLAG variant. (a) Alginate production of *P. fluorescens* SBW25 (□), SBW25 *mucA* (■), and SBW25 *mucA algE*-FLAG (▨). (b and c) TEM micrographs displaying gold particles on the outer membrane of SBW25 *mucA algE*-FLAG and no gold particles in a selected image from the tested negative controls, respectively. Each gold particle is assumed to represent an alginate biosynthesis factory. Three independent cultures were used to measure alginate production, and the error bars represent the standard deviations. The applied gold particle size was 10 nm.

Both SBW25 *mucA* and SBW25 *mucA algE*-FLAG were cultivated in DEF3 medium overnight. The FLAG-tagged AlgE protein was detectable in the whole-cell extract of strain SBW25 *mucA algE*-FLAG by Western immunoblotting analysis (Fig. 2, lane 3). This strain was also able to produce the same amount of alginate as the SBW25 *mucA* strain (Fig. 3a). Since alginate is dependent on functional protein complexes for being transported to the growth medium and not being degraded by AlgL, these results imply that in spite of the FLAG insertion, the AlgE mutant protein is expressed and can functionally replace the wild-type AlgE protein.

Establishment of a method for visualizing the AlgE-FLAG protein. Thus far, no method for quantifying the number of alginate biosynthesis complexes on the outer membrane has been reported. However, the practicality of an immunogold labeling method combined with TEM for specific and precise identification of the cellular components and structures is well established (35–37). We wanted to develop such a procedure for visualizing the AlgE-FLAG protein on the outer membrane of SBW25 *mucA algE*-FLAG. In TEM micrographs, each gold particle would represent an alginate biosynthesis factory (Fig. 3b).

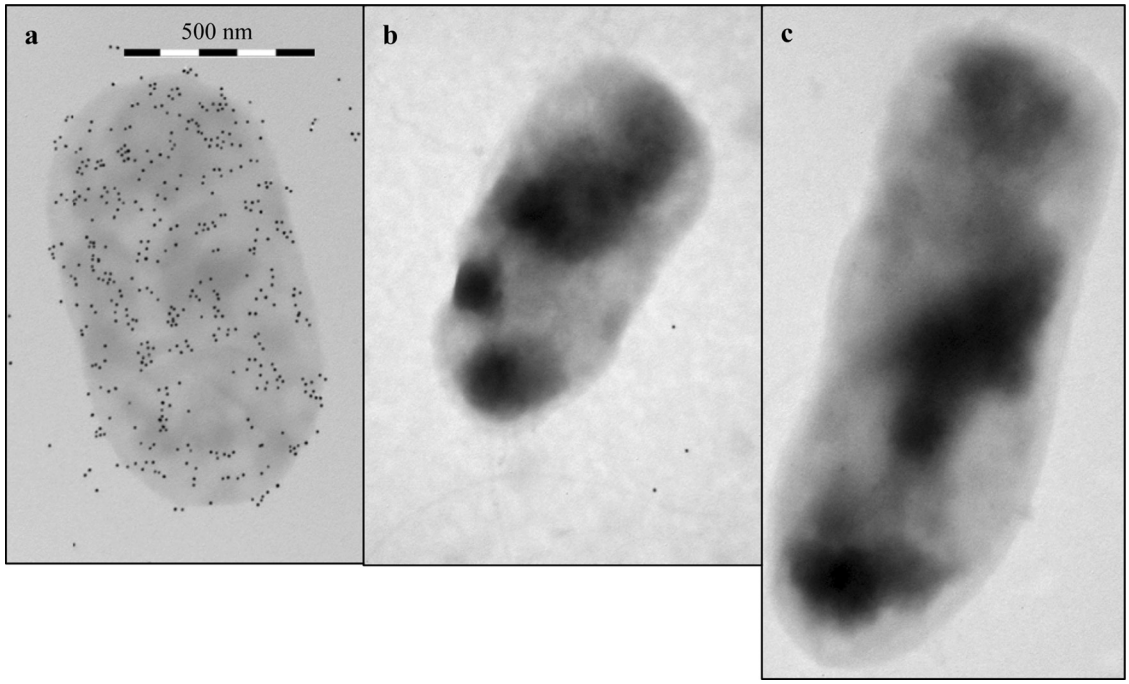

FIG 4 TEM micrographs showing the effect of other proteins expressed from *algD* operon in localization of AlgE on the outer membrane. (a) SBW25 *mucA algE*-FLAG as a positive control. (b and c) SBW25 *algE*-FLAG and SBW25::Tn*algE*-FLAG, respectively. The applied gold particle size was 10 nm.

Alginate production interfered with the procedure, since it resulted in a viscous bacterial suspension and created problems in obtaining a bacterial cell pellet. Furthermore, alginate might interfere with the labeling procedure. To avoid these problems, the samples were treated with alginate lyases before further processing.

If too little antibody is used, this would result in an underestimation of the number of alginate factories. In order to ensure that the applied antibody concentration was sufficient to saturate all gold-labeled AlgE-FLAG proteins presented on the outer membrane, experiments using double concentrated and three times more diluted antibodies were performed. This antibody saturation test results (data not shown) showed no significant difference (Student *t* test, $P > 0.05$) between the number of detected gold particles in SBW25 *mucA algE*-FLAG using the chosen antibody concentrations and that using double concentrated antibodies. There was a significant decline in counted gold particles when only one-third of the usual antibody concentration was applied (Student *t* test, $P < 0.001$).

Unspecific binding would lead to an overestimation of the number of alginate factories; therefore, three different strains were examined by TEM as negative controls to assess the potential problem of nonspecific labeling. These negative controls were: (i) SBW25 *algE*-FLAG, a derivative of the alginate-nonproducing wild-type strain SBW25 in which the alginate operon is not transcribed (38) and where the wild-type *algE* was replaced by *algE*-FLAG; (ii) SBW25 *mucA algE*-FLAG, but where the primary antibody was omitted from the immunogold labeling procedure; and (iii) SBW25 *mucA* in which the AlgE protein is not tagged, but the strain produces alginate. The reason behind using the latter control was to ensure that gold particles were not trapped by produced alginate on the cell surface. No gold particles were detected in any of these negative controls showing that both the primary and the secondary antibodies function specifically and that unspecific binding of gold particles is precluded by the procedure used (Fig. 3c). One negative control was included in all further microscopy studies.

AlgE is not localized on the outer membrane in the absence of the other proteins expressed from the *algD* operon. A model of the protein scaffold consisting of Alg8, Alg44, AlgK, AlgX, AlgG, and AlgE assembly that guides alginate through the periplasm and across the outer membrane has been proposed by several studies (Fig. 1) (17, 20, 21, 39, 40). Moreover, by using mutual stability analysis Rehman et al. (21) have shown that AlgE protein interacts with AlgK and/or AlgX. Additionally, these researchers found that AlgK and AlgX proteins are destabilized in a Δ*algE* mutant of *P. aeruginosa*. To investigate whether the localization of AlgE on the outer membrane is dependent on other Alg proteins in the complex, we used the strain SBW25::Tn*algE*-FLAG, in which *algE*-FLAG is chromosomally inserted on a transposon under the control of the inducible *Pm-G5* promoter, and the strain SBW25 *algE*-FLAG.

First, the presence of tagged AlgE protein in the whole-cell extract of the constructed strains was checked by Western immunoblotting analysis. As expected, AlgE protein was not expressed from the native promoter in SBW25 *algE*-FLAG, whereas it was expressed from the induced *Pm-G5* promoter in the transposon-based recombinant strain SBW25::Tn*algE*-FLAG (Fig. 2, lanes 6 and 1, respectively). Next, the corresponding strains were grown in minimal medium containing fructose until late exponential phase, and samples were harvested and subjected to the immunogold labeling procedure to examine the presence of AlgE in their outer membranes. SBW25 (as a negative control [data not shown]) and SBW25 *mucA algE*-FLAG (as a positive control

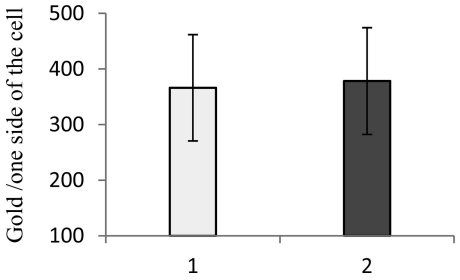

FIG 5 Number of alginate factories (gold particles) counted per one side of the cell in the absence of alginate precursor. The open and closed bars show the mean numbers of counted factories for strain SBW25 *mucA algE*-FLAG (n = 49 bacterial cells counted) and SBW25 *mucA* Δ*algC algE*-FLAG (n = 41 bacterial cells counted), respectively. Three grids were examined under TEM as technical replicates for each variant. Standard deviations are indicated by error bars. The difference between the number of gold particles counted in each case was not significant (Student t test, $P > 0.05$).

[Fig. 4a]) were also included in this experiment. Interestingly, analysis of the TEM micrographs showed no gold particles on the outer membranes of either SBW25::Tn*algE*-FLAG or SBW25 *algE*-FLAG (Fig. 4b and c). The obtained results strongly suggest that AlgE protein is not localized on the outer membrane when the other proteins encoded by the alginate biosynthesis gene cluster are not produced. The result also implied that this immunogold labeling method could be used to quantify the number of alginate factories.

Alginate factories are localized on the outer membrane even when the alginate precursor is unavailable. AlgC is essential for the alginate production, because it provides the sugar precursor mannose-1-phosphate (Man1P) for biosynthesis of alginate (41). However, Borgos et al. have shown that the other alginate biosynthesis proteins are transcribed and translated in SBW25 *mucA* Δ*algC* (25). We decided to use this strain to test whether the sugar precursor pool can play any regulatory role in establishing the alginate synthesis machinery on the outer membrane. To address this, pSM8 was used for construction of the strain SBW25 *mucA* Δ*algC algE*-FLAG, which, as expected, was nonmucoid on PIA medium. Additionally, it did not produce alginate in DEF3 minimal medium supplemented with fructose as a carbon source (data not shown). The strain did, as expected, produce AlgE-FLAG (Fig. 2, lane 5). Immunogold labeling was performed for the constructed strain, and SBW25 *mucA algE*-FLAG was used as a positive control. TEM studies revealed that alginate factories are localized on the outer membrane of both the *algC* mutant and the control strain (Fig. 5). Furthermore, there was no significant difference (Student t test, $P > 0.05$) between the number of factories in the *algC* mutant and the control. The obtained results imply that the absence of alginate precursor does not preclude assembly of the alginate factories on the outer membrane as long as the necessary genes in the *algD* operon are expressed.

Correlation between alginate production level and the number of alginate factories. To assess the relationship between the alginate production level and the number of factories located on the outer membrane, two independent cultures of SBW25 *mucA algE*-FLAG were grown in minimal medium containing fructose as the carbon source. Growth, alginate production, and number of alginate factories (detected gold particles) were quantified at certain time points covering early and late exponential and stationary phases (Fig. 6). Surprisingly, microscopy revealed the presence of a relatively high number of alginate factories located in the outer membrane even before any significant amount of alginate was produced. No clear correlation was observed between the normalized number of alginate factories per milliliter of culture (using OD_{600} values as an estimate of cell number) and the alginate production rate. The number of factories per milliliter of culture in-

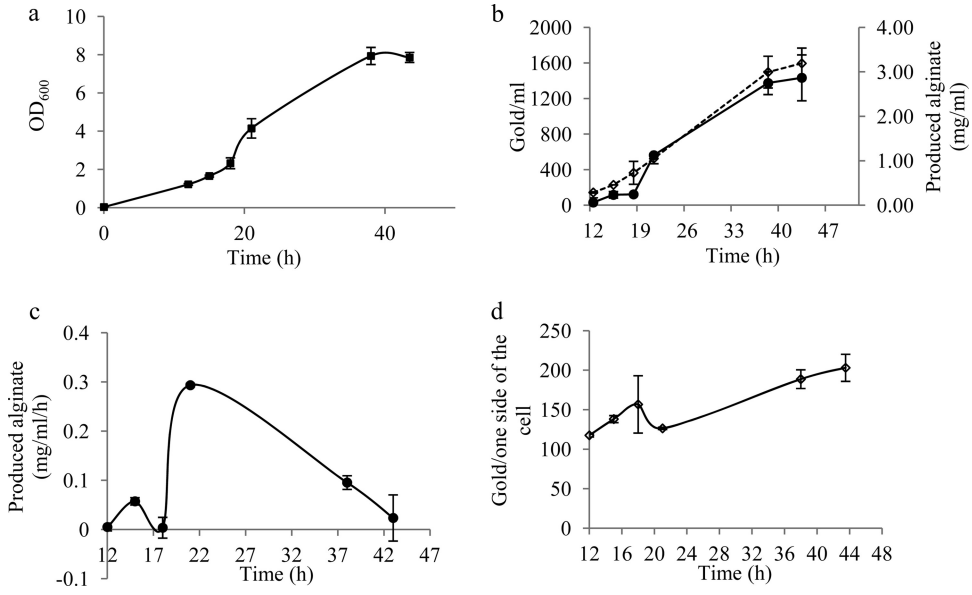

FIG 6 Correlation between alginate production level and number of produced alginate factories in SBW25 *mucA algE*-FLAG. (a) The growth profile. (b) Alginate production (●) and number of alginate factories (◇) (represented by gold particles) normalized with OD_{600} in order to be comparable with alginate production per ml. (c) Alginate production rate per hour. (d) Number of alginate factories (represented by gold particles) counted per one side of the individual cells before normalizing with OD_{600}. Experiments were performed by considering two biological and three technical (three grids per sample) replicates. At least 20 to 30 single cells were counted per each grid. Mean values are plotted on the graphs, and the error bars indicate the standard deviations.

creased with time, but this rise was not proportional to the alginate production level at time points 18 to 21 h, when there was a dramatic boost in alginate production (4.6-fold) (Fig. 6b). In addition, the number of counted alginate factories per individual cell (before normalizing with OD_{600}) was in a range of approximately 100 (at the beginning of the exponential phase) to 200 (in the stationary phase) at the defined time points (Fig. 6d). Actually, the number of factories per single cell decreased in the period 18 to 21 h; this coincided with an increased growth rate (Fig. 6a and d). These results suggest that the biosynthetic/export capacity of the existing alginate factories on the outer membrane by 18 h was sufficient to handle the significant increase in alginate production.

To better understand this relation, the amount of produced alginate per hour was also plotted. Clearly, the alginate production rate was highest in the 18- to 21-h period, whereas it decreased significantly after 21 h (Fig. 6c). This elevated production rate coincides with the growth boost at the same time point (Fig. 6a). Together, these data imply that at least in the *mucA* background alginate production depends more on the growth phase than on the number of alginate factories.

Outer membrane saturation with alginate factories. To improve the bacterial alginate production for industrial purposes, it would be interesting to investigate the capacity of the bacterial outer membrane to accommodate alginate factories. In order to assess this capacity, we decided to construct the strain SBW25 MS1 Δ*algC algE*-FLAG::TnKB60, in which the *algD* promoter that naturally controls the expression of the *algD* operon was substituted with the inducible *Pm* promoter, and the gene encoding AlgE was replaced with the one encoding AlgE-FLAG via double crossover. To be able to control alginate production in this strain, *algC* was inactivated by an in frame deletion, and a transposon (TnKB60) containing a copy of the functional *algC* under the control of the *Pm-G5* promoter was chromosomally inserted into the strain. Alginate production would be turned on in this strain upon addition of the inducer (*m*-toluate) to the culture. The idea was that using the strong inducible *Pm* promoter to control the *algD* operon would allow overexpression of the Alg proteins, thus potentially leading to an increased number of alginate factories.

The SBW25 MS1 Δ*algC algE*-FLAG::TnKB60 strain was mucoid on the PIA plate, indicating that the *alg* genes are expressed from the *Pm* promoter and that alginate is produced. The constructed recombinant strain was cultivated in DEF3 medium containing fructose, harvested after 21 h, and subjected to immunoblotting and immunogold labeling procedures. The presence of AlgE-FLAG in the whole-cell extract was confirmed by Western blotting (Fig. 2, lane 7). The TEM micrographs analysis showed that the number of alginate factories in the MS1 strain was significantly higher than that in the SBW25 *mucA algE*-FLAG (Student *t* test, $P < 0.001$). The maximum number of alginate biosynthesis factories recorded per one side of a single cell was 1,699, and the membrane integrity was not visibly compromised (Fig. 7). This finding implies that it is possible to significantly increase the number of alginate factories by overexpressing the *alg* genes.

Distribution pattern of alginate biosynthetic complexes. Visual inspection of the TEM micrographs (Fig. 3b, 4a, and 7) suggested that even though the gold particles are attached to all parts of the cell surface, the distribution pattern does not seem entirely random. In order to quantify the distribution pattern of the alginate biosynthesis factories with numerical methods, 48 images obtained from the strain SBW25 *mucA algE*-FLAG at the mid-

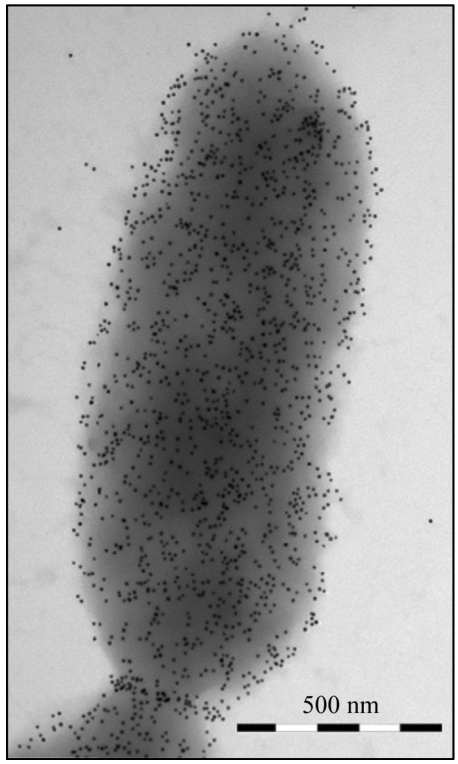

FIG 7 Overexpression of the alginate factories under the control of the inducible *Pm* promoter. A selected TEM image of strain SBW25 MS1 Δ*algC algE*-FLAG::TnKB60 is shown. The cell seems to retain its membrane integrity, while alginate factories are overproduced.

exponential growth phase were analyzed. The nearest-neighbor distance distribution indicated that more AlgE proteins had their closest neighbor at a distance of <25 nm than could have been expected if the alginate factories were randomly distributed (Fig. 8a). Similarly, a modified Ripley's K-test indicated a higher density when the distance is below 75 nm than expected by random distribution (Fig. 8b). The angle distribution quantifies the spatial coordination of the two closest neighbors of all the gold particles and shows that angles between 40 and 60 degrees are more frequently observed than would be expected from a random distribution (Fig. 8c). Ten images from stationary-phase cells were analyzed using the same algorithms, and the results were similar to those displayed in Fig. 8 (results not shown). These data all indicate that AlgE proteins (alginate factories) are clustered on the cell surface, not randomly distributed.

DISCUSSION

AlgE is an outer membrane porin through which polymerized alginate is secreted out of the cell (23). It has been shown that the alginate biosynthesis machinery components interact with each other, span the entire periplasm, and probably form a multiprotein complex guiding the newly synthesized alginate chain to the AlgE porin (22). In the present study, we developed an immunogold labeling method to detect FLAG-tagged AlgE protein as a representative of the alginate biosynthesis factory by using TEM. This method was used in several experiments designed to better understand the alginate production and factors affecting establishment of alginate factories on the outer membrane.

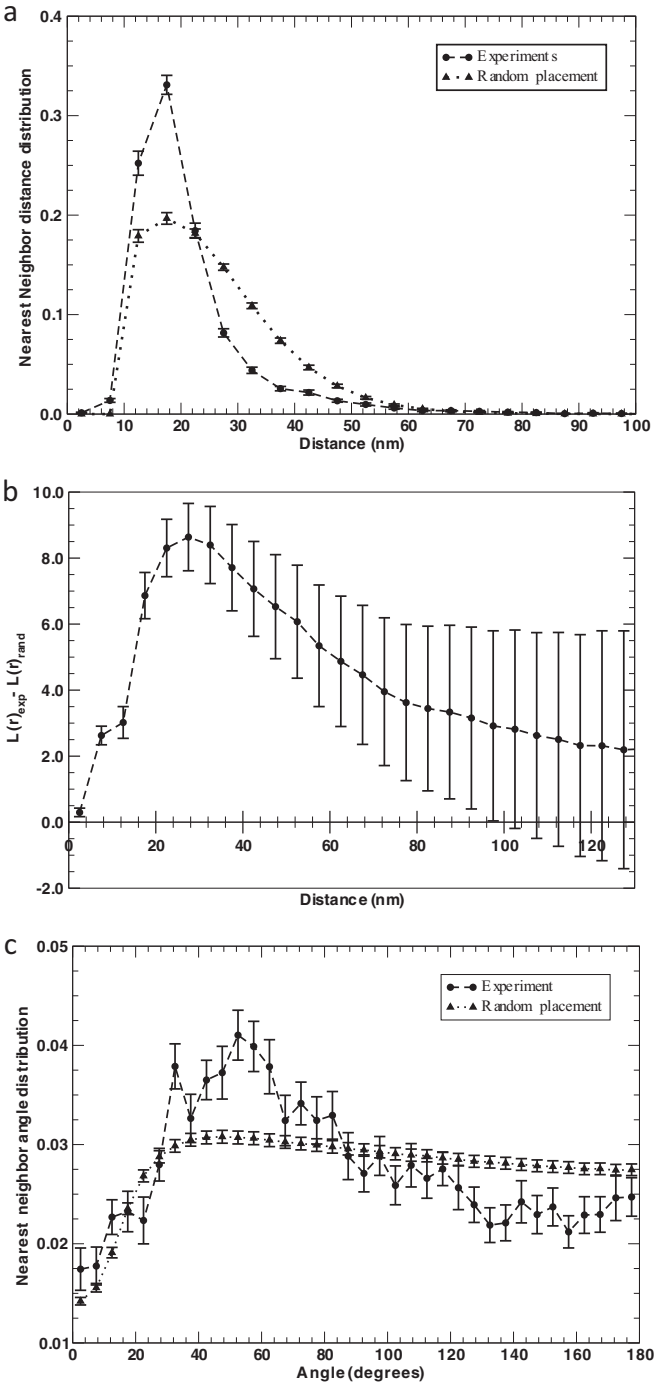

FIG 8 Distribution of gold particles on the cell surface. Gold particles on the surfaces of 48 cells were analyzed as described in Materials and Methods. (a) Distribution of nearest-neighbor distances. (b) Modified Ripley's K-test analysis for spatial distribution, where random placement constitutes a score of zero. (c) Distribution of angles between a gold particle and its two closest neighbors. The gray curves in panels a and c show the numerical results for randomly distributed particles.

No AlgE-FLAG was present on the outer membrane of the strain that did not express *alg* genes other than *algE* from the transposon (Fig. 4), while it was detected in the whole-cell extract of the respective strain by immunoblotting (Fig. 2, lane 3). This shows that AlgE expressed alone is not able to establish itself in the outer membrane. Our result is consistent with an earlier mutant stability study showing that deletion of *algX* resulted in nondetectable levels of AlgE in the envelope fraction (consisting of inner membrane, outer membrane, and associated proteins) (21).

We hypothesized that since the alginate production pathway is tightly regulated, it would be quite reasonable for the cell to save energy and material by regulating the synthesis of proteins needed for alginate production when alginate synthesis is not taking place. Surprisingly, the obtained results show that the difference between the numbers of alginate factories on the outer membrane of the Δ*algC* mutant, where the alginate biosynthesis precursor was not produced, and the alginate synthesizing control strain was not significant. This result suggests that the alginate biosynthesis complexes are produced and localized on the outer membrane of the cell regardless of the precursor availability. It is, however, possible that inactivation of *mucA* leading to constitutive availability of the sigma-factor AlgU might have changed the regulation in a way that decouples precursor biosynthesis from the establishment of alginate biosynthesis factories.

Monitoring alginate production and the number of alginate factories during various growth stages using AlgE-FLAG-based gold labeling revealed no clear correlation between the level of alginate production and the number of alginate factories (Fig. 6b and c). Moreover, a high number of alginate factories is established on the outer membrane of the single cells before any considerable amount of alginate is produced (12 h, Fig. 6c and d). This indicates that factories localized on the outer membrane are in a standby mode. The obtained data suggest that alginate production in *P. fluorescens* SBW25 *mucA* is more dependent on the precursor availability than on the number of factories. This finding is in agreement with our previous study focusing on the central carbon metabolism of *P. fluorescens*. There, we showed that inactivation of *zwf-1* (encoding glucose-6-phosphate dehydrogenase in the Entner-Doudoroff [ED] pathway) was beneficial for alginate production when glycerol was used as carbon source due to decreased carbon flow through the ED pathway and accumulation of F6P, which could be converted to alginate precursor (28).

The TEM micrographs from a strain in which the *algD* operon was overexpressed under the control of the inducible *Pm* promoter indicated that the outer membrane of the cell seems to be able to keep its integrity even when the number of alginate factories is >3-fold increased. In the future it might be possible to engineer the bacterium in such a way that the amount of precursors available for alginate production is significantly increased, and then the number of factories could become a limiting factor. Our results indicate that the number of factories can be significantly increased without affecting cell viability.

For most bacterial polysaccharides, there is little knowledge regarding the number and localization of the biosynthetic complexes. The exception is *Gluconacetobacter xylinus* (formerly *Acetobacter xylinum*), where protein clusters for cellulose biosynthesis were shown to be arranged in a line along the longitudinal axes of the cell (42). Our data show that *P. fluorescens* may contain several hundred alginate factories spread all over the cell surface. However, the statistical analyses indicated that these factories are localized in a nonrandom way.

ACKNOWLEDGMENTS

This study was supported by grants from FUGE Midt-Norge.

We thank Radka Hrudikova for constructing strain SBW25 *mucA algE*-FLAG. We are grateful to Johannes Van der Want and Nan E. Tostrup Skogaker for their advice on the microscopy methods.

REFERENCES

1. **Gimmestad M, Sletta H, Ertesvåg H, Bakkevig K, Jain S, Suh S-J, Skjåk-Bræk G, Ellingsen TE, Ohman DE, Valla S.** 2003. The *Pseudomonas fluorescens* AlgG protein, but not its mannuronan C5-epimerase activity, is needed for alginate polymer formation. J Bacteriol **185:**3515–3523.
2. **Draget KI, Smidsrød O, Skjåk-Bræk G.** 2005. Alginates from algae. Biopolymers online. Wiley-VCH Verlag GmbH & Co, Berlin, Germany.
3. **Hay ID, Rehman ZU, Moradali MF, Wang Y, Rehm BHA.** 2013. Microbial alginate production, modification and its applications. Microb Biotechnol **6:**637–650.
4. **Govan JRW, Nelson JW.** 1992. Microbiology of lung infection in cystic fibrosis. Br Med Bull **48:**912–930.
5. **Chitnis CE, Ohman DE.** 1993. Genetic analysis of the alginate biosynthetic gene cluster of *Pseudomonas aeruginosa* shows evidence of an operonic structure. Mol Microbiol **8:**583–593.
6. **Paletta JL, Ohman DE.** 2012. Evidence for two promoters internal to the alginate biosynthesis operon in *Pseudomonas aeruginosa*. Curr Microbiol **65:**770–775. http://dx.doi.org/10.1007/s00284-012-0228-y.
7. **Ye RW, Zielinski NA, Chakrabarty AM.** 1994. Purification and characterization of phosphomannomutase/phosphoglucomutase from *Pseudomonas aeruginosa* involved in biosynthesis of both alginate and lipopolysaccharide. J Bacteriol **176:**4851–4857.
8. **May TB, Shinabarger D, Boyd A, Chakrabarty AM.** 1994. Identification of amino acid residues involved in the activity of phosphomannose isomerase-guanosine 5′-diphospho-D-mannose pyrophosphorylase: a bifunctional enzyme in the alginate biosynthetic pathway of *Pseudomonas aeruginosa*. J Biol Chem **269:**4872–4877.
9. **Roychoudhury S, May TB, Gill JF, Singh SK, Feingold DS, Chakrabarty AM.** 1989. Purification and characterization of guanosine diphospho-D-mannose dehydrogenase. A key enzyme in the biosynthesis of alginate by *Pseudomonas aeruginosa*. J Biol Chem **264:**9380–9385.
10. **Lessie TG, Phibbs JPV.** 1984. Alternative pathways of carbohydrate utilization in pseudomonads. Annu Rev Microbiol **38:**359–388.
11. **Oglesby LL, Jain S, Ohman DE.** 2008. Membrane topology and roles of *Pseudomonas aeruginosa* Alg8 and Alg44 in alginate polymerization. Microbiology **154:**1605–1615. http://dx.doi.org/10.1099/mic.0.2007/015305-0.
12. **Franklin MJ, Chitnis CE, Gacesa P, Sonesson A, White DC, Ohman DE.** 1994. *Pseudomonas aeruginosa* AlgG is a polymer level alginate C5-mannuronan epimerase. J Bacteriol **176:**1821–1830.
13. **Baker P, Ricer T, Moynihan PJ, Kitova EN, Walvoort MTC, Little DJ, Whitney JC, Dawson K, Weadge JT, Robinson H, Ohman DE, Codée JDC, Klassen JS, Clarke AJ, Howell PL.** 2014. *Pseudomonas aeruginosa* SGNH hydrolase-like proteins AlgJ and AlgX have similar topology but separate and distinct roles in alginate acetylation. PLoS Pathog **10:**e1004334. http://dx.doi.org/10.1371/journal.ppat.1004334.
14. **Franklin MJ, Ohman DE.** 2002. Mutant analysis and cellular localization of the AlgI, AlgJ, and AlgF proteins required for O acetylation of alginate in *Pseudomonas aeruginosa*. J Bacteriol **184:**3000–3007.
15. **Franklin MJ, Ohman DE.** 1996. Identification of *algI* and *algJ* in the *Pseudomonas aeruginosa* alginate biosynthetic gene cluster which are required for alginate O acetylation. J Bacteriol **178:**2186–2195.
16. **Bakkevig K, Sletta H, Gimmestad M, Aune R, Ertesvåg H, Degnes K, Christensen BE, Ellingsen TE, Valla S.** 2005. Role of the *Pseudomonas fluorescens* alginate lyase (AlgL) in clearing the periplasm of alginates not exported to the extracellular environment. J Bacteriol **187:**8375–8384.
17. **Jain S, Ohman DE.** 1998. Deletion of *algK* in mucoid *Pseudomonas aeruginosa* blocks alginate polymer formation and results in uronic acid secretion. J Bacteriol **180:**634–641.
18. **Robles-Price A, Wong TY, Sletta H, Valla S, Schiller NL.** 2004. AlgX is a periplasmic protein required for alginate biosynthesis in *Pseudomonas aeruginosa*. J Bacteriol **186:**7369–7377.
19. **Hay ID, Rehman ZU, Rehm BH.** 2010. Membrane topology of outer membrane protein AlgE, which is required for alginate production in *Pseudomonas aeruginosa*. Appl Environ Microbiol **76:**1806–1812. http://dx.doi.org/10.1128/AEM.02945-09.
20. **Jain S, Franklin MJ, Ertesvåg H, Valla S, Ohman DE.** 2003. The dual roles of AlgG in C-5-epimerization and secretion of alginate polymers in *Pseudomonas aeruginosa*. Mol Microbiol **47:**1123–1133.
21. **Rehman ZU, Wang Y, Moradali MF, Hay ID, Rehm BHA.** 2013. Insights into the assembly of the alginate biosynthesis machinery in *Pseudomonas aeruginosa*. Appl Environ Microbiol **79:**3264–3272. http://dx.doi.org/10.1128/AEM.00460-13.
22. **Moradali MF, Donati I, Sims IM, Ghods S, Rehm BH.** 2015. Alginate polymerization and modification are linked in *Pseudomonas aeruginosa*. mBio **6:**e00453-15. http://dx.doi.org/10.1128/mBio.00453-15.
23. **Tan J, Rouse SL, Li D, Pye VE, Vogeley L, Brinth AR, El Arnaout T, Whitney JC, Howell PL, Sansom MS, Caffrey M.** 2014. A conformational landscape for alginate secretion across the outer membrane of *Pseudomonas aeruginosa*. Acta Crystallogr D Biol Crystallogr **70:**2054–2068. http://dx.doi.org/10.1107/S1399004714001850.
24. **Jain S, Ohman DE.** 2005. Role of an alginate lyase for alginate transport in mucoid *Pseudomonas aeruginosa*. Infect Immun **73:**6429–6436.
25. **Borgos SEF, Bordel S, Sletta H, Ertesvåg H, Jakobsen Ø, Bruheim P, Ellingsen TE, Nielsen J, Valla S.** 2013. Mapping global effects of the anti-sigma factor MucA in *Pseudomonas fluorescens* SBW25 through genome-scale metabolic modeling. BMC Syst Biol **7:**1–15. http://dx.doi.org/10.1186/1752-0509-7-19.
26. **Schurr MJ, Yu H, Martinez-Salazar JM, Boucher JC, Deretic V.** 1996. Control of AlgU, a member of the sigma E-like family of stress sigma factors, by the negative regulators MucA and MucB and *Pseudomonas aeruginosa* conversion to mucoidy in cystic fibrosis. J Bacteriol **178:**4997–5004.
27. Reference deleted.
28. **Maleki S, Mærk M, Valla S, Ertesvåg H.** 2015. Mutational analyses of glucose dehydrogenase and glucose-6-phosphate dehydrogenase genes in *Pseudomonas fluorescens* reveal their effects on growth and alginate production. Appl Environ Microbiol **81:**3349–3356. http://dx.doi.org/10.1128/AEM.03653-14.
29. **Ertesvåg H, Skjåk-Bræk G.** 1999. Modification of alginate using mannuronan C-5-epimerases. Methods Biotechnol **10:**71–78. http://dx.doi.org/10.1007/978-1-59259-261-6_6.
30. **Østgaard K.** 1992. Enzymatic microassay for the determination and characterization of alginates. Carbohydr Polym **19:**51–59.
31. **Slootstra JW, Kuperus D, Plückthun A, Meloen RH.** 1997. Identification of new tag sequences with differential and selective recognition properties for the anti-FLAG monoclonal antibodies M1, M2, and M5. Mol Divers **2:**156–164.
32. **Gimmestad M, Sletta H, Karunakaran P, Bakkevig K, Ertesvåg H, Ellingsen TE, Skjåk-Bræk G, Valla S.** May 2014. New mutant strains of *Pseudomonas fluorescens* and variants thereof, methods of their production, and uses thereof in alginate production. European patent WO 2004/011628.
33. **Laemmli UK.** 1970. Cleavage of structural proteins during the assembly of the head of bacteriophage T4. Nature **227:**680–685.
34. **Hess ST, Kumar M, Verma A, Farrington J, Kenworthy A, Zimmerberg J.** 2005. Quantitative electron microscopy and fluorescence spectroscopy of the membrane distribution of influenza hemagglutinin. J Cell Biol **169:**965–976.
35. **Kaur R, Dikshit KL, Raje M.** 2002. Optimization of immunogold labeling TEM: an ELISA-based method for evaluation of blocking agents for quantitative detection of antigen. J Histochem Cytochem **50:**863–873.
36. **Levine MM, Ristaino P, Marley G, Smyth C, Knutton S, Boedeker E, Black R, Young C, Clements ML, Cheney C.** 1984. Coli surface antigens 1 and 3 of colonization factor antigen II-positive enterotoxigenic *Escherichia coli*: morphology, purification, and immune responses in humans. Infect Immun **44:**409–420.
37. **Schaber JA, Triffo WJ, Suh SJ, Oliver JW, Hastert MC, Griswold JA, Auer M, Hamood AN, Rumbaugh KP.** 2007. *Pseudomonas aeruginosa* forms biofilms in acute infection independent of cell-to-cell signaling. Infect Immun **75:**3715–3721.
38. **Rainey PB, Bailey MJ.** 1996. Physical and genetic map of the *Pseudomonas fluorescens* SBW25 chromosome. Mol Microbiol **19:**521–533.
39. **Rehman ZU, Rehm BHA.** 2013. Dual roles of *Pseudomonas aeruginosa* AlgE in secretion of the virulence factor alginate and formation of the secretion complex. Appl Environ Microbiol **79:**2002–2011. http://dx.doi.org/10.1128/AEM.03960-12.
40. **Keiski C-L, Harwich M, Jain S, Neculai AM, Yip P, Robinson H, Whitney JC, Riley L, Burrows LL, Ohman DE, Howell PL.** 2010. AlgK is a TPR-containing protein and the periplasmic component of a novel

exopolysaccharide secretin. Structure **18:**265–273. http://dx.doi.org/10.1016/j.str.2009.11.015.
41. **Zielinski NA, Chakrabarty AM, Berry A.** 1991. Characterization and regulation of the *Pseudomonas aeruginosa algC* gene encoding phosphomannomutase. J Biol Chem **266:**9754–9763.
42. **Brown RM, Jr, Willison JH, Richardson CL.** 1976. Cellulose biosynthesis in *Acetobacter xylinum*: visualization of the site of synthesis and direct measurement of the in vivo process. Proc Natl Acad Sci U S A **73:**4565–4569.
43. **Simon R, Priefer U, Pühler A.** 1983. A broad host range mobilization system for *in vivo* genetic engineering: transposon mutagenesis in Gram-negative bacteria. Biotechnology **1:**784–791.
44. **de Lorenzo V, Cases I, Herrero M, Timmis KN.** 1993. Early and late response of TOL promoters to pathway inducers: identification of post-exponential promoters in *Pseudomonas putida* with *lacZ-tet* bicistronic reporters. J Bacteriol **175:**6902–6907.
45. **Keen NT, Tamaki S, Kobayashi D, Trollinger D.** 1988. Improved broad-host-range plasmids for DNA cloning in Gram-negative bacteria. Gene **70:**191–197.